

VisTR: Visualizations as Representations for Time-series Table Reasoning

Jianing Hao, Zhuowen Liang, Chunting Li, Yuyu Luo, Jie Li, Wei Zeng *Member, IEEE*,

Abstract—Time-series table reasoning interprets temporal patterns and relationships in data to answer user queries. Despite recent advancements leveraging large language models (LLMs), existing methods often struggle with pattern recognition, context drift in long time-series data, and the lack of visual-based reasoning capabilities. To address these challenges, we propose *VisTR*, a framework that places visualizations at the core of the reasoning process. Specifically, *VisTR* leverages visualizations as *representations* to bridge raw time-series data and human cognitive processes. By transforming tables into fixed-size visualization references, it captures key trends, anomalies, and temporal relationships, facilitating intuitive and interpretable reasoning. These visualizations are aligned with user input, *i.e.*, charts, text, and sketches, through a fine-tuned multimodal LLM, ensuring robust cross-modal alignment. To handle large-scale data, *VisTR* integrates pruning and indexing mechanisms for scalable and efficient retrieval. Finally, an interactive visualization interface supports seamless multimodal exploration, enabling users to interact with data through both textual and visual modalities. Quantitative evaluations demonstrate the effectiveness of *VisTR* in aligning multimodal inputs and improving reasoning accuracy. Case studies further illustrate its applicability to various time-series reasoning and exploration tasks.

Index Terms—Table reasoning, visualization representation, multimodal LLMs.

I. INTRODUCTION

TIME-series tabular data are ubiquitous, forming the backbone of decision-making processes across domains such as finance, healthcare, and logistics [1], [2]. These datasets record sequential information over time, enabling the discovery of temporal trends and interesting relationships that drive actionable insights [3], [4]. Time-series table reasoning, a key task in this context, focuses on interpreting these patterns to answer user queries, such as “What is the price trend of Apple during March?” (see Fig. 1-Q1). Intuitively, effectively addressing this task requires a comprehensive understanding of not only the raw tabular data but also the temporal trends, interrelationships among data points, and alignment with the specific context of user queries [5].

Recently, large language models (LLMs) have demonstrated promising capabilities in extending their applications to table

reasoning tasks [6]–[8]. These methods can be broadly categorized into: (1) *generic table reasoning*, where pre-trained models or LLMs directly generate answers, often enhanced by techniques such as prompt design [9], [10], iterative reasoning, or flexible tabular formats [11], [12]; and (2) *program-aided table reasoning* which employs executable query languages (*e.g.*, SQL, SPARQL, or Python) to bridge user queries with answers derived from tabular data [13]–[15].

Limitations of Existing Solutions. Despite these advances, existing solutions exhibit limitations, as illustrated in Fig. 1.

(1) *Limited Pattern Recognition.* LLMs often struggle to identify and interpret temporal data patterns, such as trends, peaks, or valleys [1], [16]. For example, in Q1 of Fig. 1, an LLM-based approach misinterprets Apple’s stock prices as exhibiting a “declining trend” rather than recognizing the correct two-peak trend.

(2) *Challenges with Long Time-series Data.* LLMs often lose focus and context when reasoning over long time-series data, leading to errors caused by “LLM drift” [17]. In Q2 of Fig. 1, an LLM-based method erroneously identifies Google’s stock price bottom as occurring “at the beginning” rather than pinpointing the correct date.

(3) *Inability to Perform Visual-based Reasoning.* Existing LLMs cannot effectively reason over external visual references, limiting their ability to align time-series data with visual patterns [18]. For example, in Q3 of Fig. 1, an LLM-based method fails to determine whether Tesla’s stock price exhibits a similar pattern to a user-provided chart, demonstrating the gap in visual-based reasoning capabilities.

Rethinking: How Can Visualization Help? Visualizations, such as line and bar charts, offer an intuitive means of representing time-series data by highlighting trends, outliers, and temporal relationships [19], [20]. They act as a cognitive bridge, enabling humans to discern patterns that might otherwise remain obscured in raw time-series data.

Despite their potential, existing table reasoning methods largely overlook the use of *visualizations as proxies* for reasoning. Instead, they rely heavily on text-based reasoning, which struggles to emulate *human-like* cognitive processes and often fails in tasks requiring complex pattern recognition and context alignment with user intentions.

Our Proposal. Inspired by the ability of visualizations to simplify complex patterns and align with human cognitive processes, we propose a new framework that integrates visualizations as *representations* into multimodal large language

J. Hao, C. Li, Y. Luo, and W. Zeng are with the Hong Kong University of Science and Technology (Guangzhou). Y. Luo and W. Zeng are also with the Hong Kong University of Science and Technology Email: {jhao768@connect, cli087@connect, yuyuluo@, weizeng@}.hkust-gz.edu.cn

Z. Liang is with the South China University of Technology. simon-liang484@gmail.com

J. Li is with the Tianjin University. jie.li@tju.edu.cn

W. Zeng is the corresponding author.

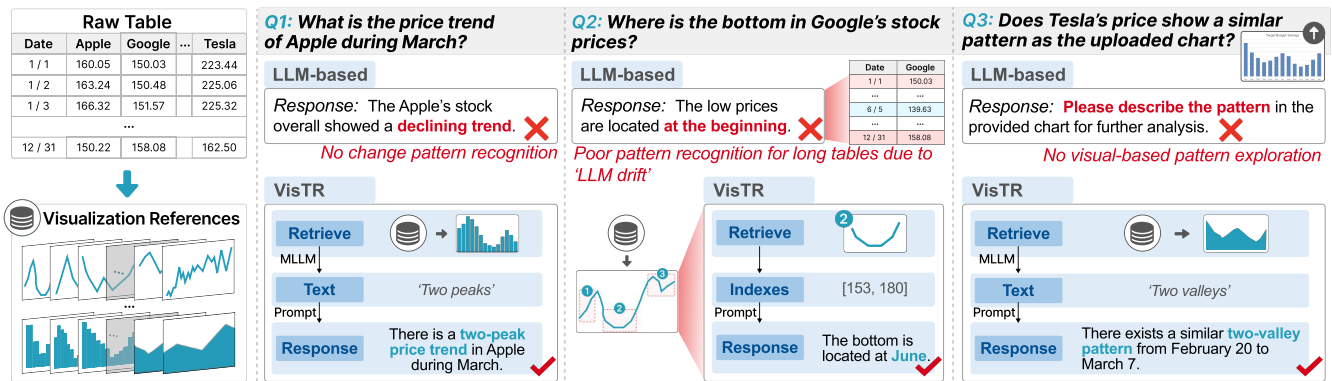


Fig. 1. *VisTR* leverages visualizations as the *representations* to bridge the gap between time-series data and user queries. *VisTR* enhances existing LLM-based table reasoning methods by enabling robust data change pattern recognition (Q1), improving pattern recognition for long-term series (Q2), and facilitating visual-based pattern exploration (Q3).

models (MLLMs). **Our goal** is to achieve the best of both worlds by combining the interpretability and intuitive pattern recognition offered by visualizations with the reasoning and generative capabilities of LLMs, thereby enhancing both the accuracy and usability of time-series table reasoning systems. The **key idea** of our framework is to transform *time-series data* into a set of meaningful and insightful visualizations, termed *visualization references*. These references act as concise representations of the data, capturing essential insights such as trends, anomalies, and temporal relationships, while aligning closely with user intentions for reasoning tasks.

Framework Overview. At its core, the framework transforms input tables into fixed-size visualization references that capture key trends, anomalies, and temporal relationships, enabling a comprehensive and interpretable representation of both long- and short-term data patterns. To achieve this, the framework begins by decomposing tables into smaller, meaningful data facets, each representing a subset of the table’s temporal or structural characteristics. These facets are then converted into visualizations, ensuring a rich and diverse representation of the data. Second, to align user intentions with these visualization references, the framework incorporates a fine-tuned MLLM that constructs a unified embedding space for multimodal inputs, including charts, text, and hand-drawn sketches. A novel cross-modal dataset is developed to enhance alignment precision, combining augmented chart-text pairs with user-labeled chart-sketch pairs. By extending the CLIP model [21] with advanced loss functions, *e.g.*, a two-level cross-entropy loss and a bidirectional triplet ranking loss, the framework ensures accurate and consistent alignment across modalities, bridging the gap between user inputs and relevant visualizations. Third, given the large-scale visualization references generated from extensive datasets, the framework incorporates a pruning and indexing mechanism to enhance scalability and retrieval efficiency. Less informative visualizations are filtered out, while the remaining embeddings are indexed in a vector database, enabling fast and accurate retrieval during user interactions. Finally, the framework integrates these components into an intuitive visualization interface supporting seamless multimodal interaction. Using a “decomposing-execution-filling” strategy, user queries are broken into retrieval tasks,

linked to textual descriptions generated by the fine-tuned MLLM, and reintegrated into the table for final responses. This interface enables interactive exploration through charts, text, and sketches. Our framework offers several key advantages over existing LLM-based table reasoning methods.

(1) *Enhanced Pattern Recognition Across Time Scales.* Visualization references effectively capture both short- and long-term data change patterns, making it easier to identify nuanced temporal trends. For example, in Fig. 1(Q1), the “two-peak” price trend of Apple during March is clearly represented, overcoming the limitations of purely text-based approaches.

(2) *Mitigating Context Drift in Long Time-series.* Fixed-size visualization references condense data patterns, mitigating context drift issues in long time-series reasoning. For example, in Fig. 1(Q2), a year-long stock price change is condensed into a single visualization, making it easy to pinpoint the price bottom without losing contextual accuracy.

(3) *Intuitive Multimodal Interaction.* Integrating visualizations as representations enables natural, multimodal data exploration by aligning with human cognitive processes. For example, Fig. 1(Q3) shows how combining textual descriptions with charts improves query interpretation and reduces reliance on raw time-series data [22].

In summary, we make the following contributions:

- **Framework.** We propose *VisTR* that leverages visualizations as *representations* to enhance time-series table reasoning. This new framework enables robust pattern recognition and intuitive exploration for time-series data.
- **Multimodal Visualization Alignment.** We finetune an effective MLLM that learns a joint embedding space across three modalities, *i.e.*, charts, text, and hand-drawn sketches. This alignment bridges user intentions with visualization references, enabling users to explore time-series tables through multimodal interactions.
- **Prototype Construction.** We implement a prototype system that facilitates reasoning and exploration of large-scale time-series tables.
- **Evaluation.** We conduct extensive evaluations, including quantitative experiments and case studies, to demonstrate the effectiveness and usability of *VisTR*. All datasets, fine-tuned models, and evaluation results are available at <https://osf.io/yun9d/>.

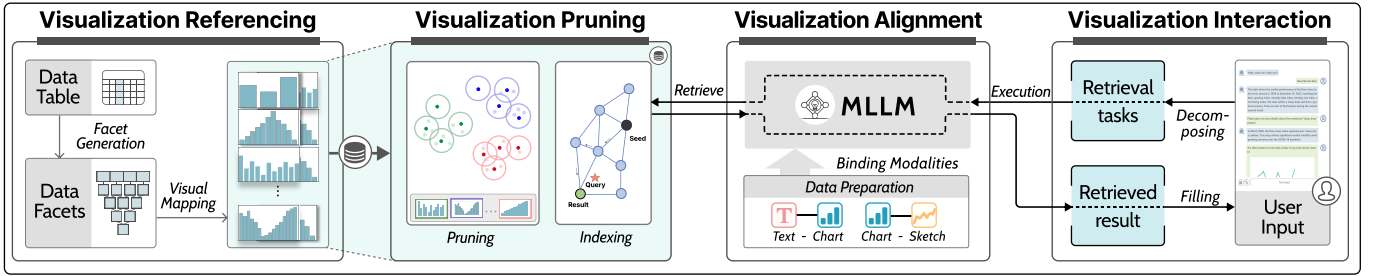


Fig. 2. An overview of the proposed framework, which mainly contains four main modules of *visualization referencing*, *visualization pruning*, *visualization alignment*, and *visualization interaction*.

II. RELATED WORK

A. Table Reasoning

Table reasoning integrated with natural language (NL) interfaces enables lay users to explore tabular data effortlessly, supporting complex tasks such as fact verification [23] and question answering [24]. Existing LLM-based table reasoning methods can be categorized into *generic table reasoning* and *program-aided table reasoning* [11]. Generic reasoning methods employ LLMs to interpret and respond to free-form NL queries by generating answers directly from tables [9]. However, due to the complexity of table structure, these methods struggle with large tables and offer limited explainability because of their end-to-end nature. Program-aided table reasoning utilizes executable query languages, such as SQL, to form a structured and accountable bridge between user queries and the derived answers [25]–[27]. Recent research has mostly focused on leveraging LLMs to transform complex user utterances into SQL queries with data context awareness [13], using prompt engineering [28], chain-of-thought [11], [29], and pre-training techniques [30]. However, program-aided approaches encounter intricate limitations due to their reliance on query language. First, SQLs primarily cater to numerical queries from tables but lack support of analytical functionality [16], overlooking data change patterns. Second, when confronted with large tables, LLMs may encounter drift issues [17] while accessing information in the middle of long contexts. Moreover, in many scenarios, relying solely on textual inputs limits the expression of non-verbal intentions, such as hand-drawn sketches, reducing the flexibility of user interactions.

To overcome these limitations, this work introduces a novel framework that leverages visualizations as a *representation* between tables and user intentions. Our inspiration is that visualizations can depict intuitive data patterns and illustrate complex underlying processes [31], aiding swift and effective interpretation by users [32]. However, this approach also presents challenges to be tackled. First, tabular data typically encompass numerous features, leading to a plethora of potential visualizations [33], [34] that complicate interactive interactions. Second, there are no direct approaches available to connect free-form user queries with visualizations.

B. Multimodal Visualization Alignment

Given that visualizations are inherently stored as images, we opt to leverage emerging MLLMs to embed visualization images and facilitate multimodal user interactions. In

recent years, significant advancements have been made in utilizing vision-language models for chart-based tasks, such as CQA [35]–[37], chart retrieval [38] and generation [39], [40]. Though CQA models can provide answers for user utterances, these models only support text-chart interactions, lacking the capability for cross-modal interactions involving multiple modalities such as text, chart, and sketch preferred by laymen [41]. Furthermore, these models are not specifically designed for effectively recognizing data change patterns (see Sect. VI-A), a gap that this work seeks to fill in the context of table reasoning. To this end, we choose to construct a novel vision-language model with an innovative visualization alignment strategy. Most existing multimodal data alignment methods rely on contrastive language-image pre-training (CLIP) [21], which has demonstrated its adaptability and proficiency across various tasks [42]–[44], highlighting the effectiveness of joint embedding spaces. However, training an effective CLIP-based alignment model for visualizations is non-trivial. First, this task involves aligning more than two modalities, including text, hand-drawn sketches, and various types of charts, whereas the original CLIP model was designed to support text-image alignment. To encompass more modalities, we adopt joint embedding strategies that leverage charts as naturally aligned supervision and emergent alignments to unify other modalities [45]. This approach allows us to prepare paired data only for chart-text and chart-sketch, rather than other pairings such as sketch-text. Second, the effectiveness of CLIP is largely attributed to its extensive training on vast (natural) image-text datasets, whereas there is a lack of suitable training datasets for the task in this work. Efforts have been made to construct datasets for promoting deep learning models for chart-text (*e.g.*, [35], [46]), chart-chart (*e.g.*, [47]–[49]), chart-sketch (*e.g.*, [41], [50], [51]) similarity measurement. However, these different modalities are not inherently unified in one model, and many of these datasets are not specifically designed for recognizing data change patterns. To address this gap, we utilize data augmentation and user labeling strategies to supplement existing datasets in training the multimodal visualization alignment model.

C. Visualization Storage, Indexing, and Retrieval

To comprehensively represent tabular data, our approach will generate a large number of visualization references and encode them into vector representations, thus raising new challenges for efficiently storing, indexing, and retrieving them. With the recent advancements in Vector Database Management

Systems (VDBMS) [52], there is potential to meet our demand. VDBMSs are specifically designed for managing high-dimensional data, such as embeddings, offering sophisticated storage, indexing, query processing, and query optimization capabilities [53]. Their ability to perform efficient similarity searches in high-dimensional spaces makes them particularly suited for tasks involving the retrieval of embeddings based on content or semantic similarity. This supports various applications such as information retrieval, e-commerce, and recommendation platforms [54], [55]. Existing VDBMS can be roughly categorized into two types: *native* systems and *extended* systems [52]. The former, such as Chroma [56] and EuclidesDB [57], are tailored for vector data management, while the latter, such as AnalyticDB-V [58], are built on top of an existing data management system.

In this work, we first introduce a visualization pruning method to filter out less informative visualizations, and effectively reduce storage demands while maintaining the quality of stored visualizations. We then integrate Chroma [56] into *VisTR* and utilize an efficient graph-based index to store and index the large collection of visualization references. An *Approximate k-Nearest Neighbors* (ANN) algorithm is incorporated to retrieve visualizations. The combination of pruning with indexing allows for quick retrieval and handling timely user queries.

III. THE VISUALIZATION ENHANCED FRAMEWORK

The visualization enhanced framework consists of four modules: *visualization alignment*, *visualization referencing*, *visualization pruning*, and *visualization interaction*, as shown in Fig. 2.

Visualization Alignment. As the cornerstone of our framework, a MLLM is fine-tuned to establish a single joint embedding space for various modalities, including chart (C), text (T), and sketch (S). To address the issue of a lack of suitable training data, we first curate a new dataset with chart-text pairings augmented from existing Chart-to-Text dataset [46], and chart-sketch pairings through user labeling. Utilizing the pre-trained CLIP [21], we fine-tune a multimodal LLM on our composite dataset, employing a Transformer [59] for text modality, and ViT [60] encoders for chart and sketch modalities, respectively. To achieve alignment across modalities within the joint embedding space, we implement a bidirectional hinge-based triplet ranking loss function and a two-level cross-entropy loss function. Through this process, we successfully align the three modalities and yield strong performance across four evaluation metrics surpassing a threshold of 0.85. A detailed description of the module is provided in Sect. IV.

Visualization Referencing. In the *visualization referencing* module, we generate visualization references that comprehensively capture key data patterns inherent in an input table. This module employs a two-stage approach that first decomposes the input table D into data facets, which are then mapped into fixed-size visualization references. The description of this module is detailed in Sect. V-A.

Visualization Pruning. In the *visualization pruning* module, we introduce pruning and indexing techniques to enable

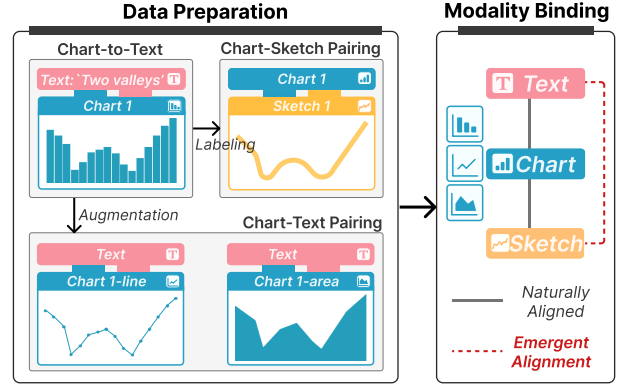


Fig. 3. An overview of *visualization alignment* module, which contains data preparation for chart-text and chart-sketch pairings, and achieves the alignment for chart, sketch, and text modalities.

timely visualization reference retrieval. Specifically, visualization pruning works by filtering out less informative visualization references by measuring the similarity between visualization vectors using Euclidean distance and applying a pruning threshold. This process reduces the number of stored references while preserving essential data change patterns. Concurrently, visualization indexing leverages an open-source vector database, Chroma [56], to efficiently store and retrieve visualization references. Here, we use the fine-tuned MLLM to transform all the pruned visualization references into 512-dimensional vectors, which are then indexed by Chroma for rapid and accurate follow-up retrieval. This combination of pruning and indexing ensures *VisTR* can swiftly manage and retrieve massive visualization references with precision. This module is detailed in Sect. V-B.

Visualization Interaction. For *visualization interaction*, we introduce a “decomposing-execution-filling” strategy to enable the connection of multimodal user queries with the stored embeddings of visualization references. Specifically, the user query is first decomposed into a visualization retrieval task. Second, the retrieval task is executed in Chroma to get a retrieved visualization reference. Afterward, with the help of the fine-tuned MLLM, the corresponding trend word of the retrieved visualization reference is generated and then filled into the textual response to the user. An interactive visual interface with multiple views and rich interactions is also developed to support the iterative table reasoning process, transitioning from abstract to detailed exploration, as detailed in Sect. V-C.

IV. MULTIMODAL VISUALIZATION ALIGNMENT

We set out to establish a MLLM that aligns visualization modalities of chart, sketch, and text in a single joint embedding space. This section presents the data preparation, including data augmentation and user labeling strategies, to address the issue of lacking training dataset (Sect. IV-A), followed by modality binding for establishing a joint embedding space that binds chart, sketch, and text modalities together (Sect. IV-B). In the end, we present the implementation details (Sect. IV-C).

A. Data Preparation

To train the multimodal visualization alignment model, we need to first prepare a dataset containing user intentions, which is not covered by current open-sourced datasets. To achieve the alignment of sketches, charts, and text, we employ two strategies to construct the training data: (1) data augmentation for chart-text pairing, and (2) user labeling for chart-sketch pairing. Fig. 3 uses an example to illustrate the two data preparation strategies.

(1) **Data augmentation for chart-text pairing.** To make up for the lack of data change pattern recognition in the existing table reasoning works, we should focus on the charts that describe data change patterns. We first survey existing chart-text datasets, and find that different textual contents are contained for different downstream tasks. We select the Chart-to-Text dataset [46] as the original dataset because it offers textual descriptions and underlying data tables for charts. Since we mainly focus on the data change patterns existing in charts, we filter the trend words from the textual descriptions. Initially, we manually extracted the contained trend words in five textual descriptions. These five descriptions with their corresponding trend words served as prompts for GPT-4 to perform an accurate trend word filtering process on the large Chart-to-Text dataset. In the filtering process, we find diversity in both trend words and charts. For trend words, we notice that different trend words in textual descriptions may indicate the same change pattern, such as ‘increasing’, ‘upward’, and ‘rising’, which typically indicate an upward trend in the data. We construct a dictionary of similar trend words, grouping the words describing similar patterns into the same category, and we get 23 categories ($N_T = 23$) of trend words. For charts, we find that three chart types: line, bar, and area charts, are widely chosen to describe the data change patterns. To balance the number of three chart types contained in the final chart-text pairing dataset, we supplement each filtered chart with two other types of charts. In total, we create a total of 5,010 chart-text pairings.

(2) **User labeling for chart-sketch pairing.** When searching for hand-drawn sketch datasets associated with charts, we encounter a significant challenge: existing public sketch datasets do not adequately meet our need to convey users’ intentions about data change patterns. Specifically, the existing sketch datasets are not suitable for our work due to the following points. 1) Most open-sourced large human sketch datasets *e.g.*, [61], mainly focus on how users draw objects, rather than on visualizations. 2) LADV [62] and VisAtlas [49] are designed for chart type matching based on pixel-wise similarity, but not the contained data change patterns. 3) Sketch query systems, such as Qetch [41], focus on data-level similarities between hand-drawn sketches and the raw data, which lacks correspondence with fixed-size charts.

In order to collect chart-sketch pairings that conform to users’ intentions about data change patterns, we invite users to draw sketches and evaluate chart-sketch pairings. 1) *Setup.* Every user is given a training session to get familiar with experimental procedures and hand-drawn board operations. 2)

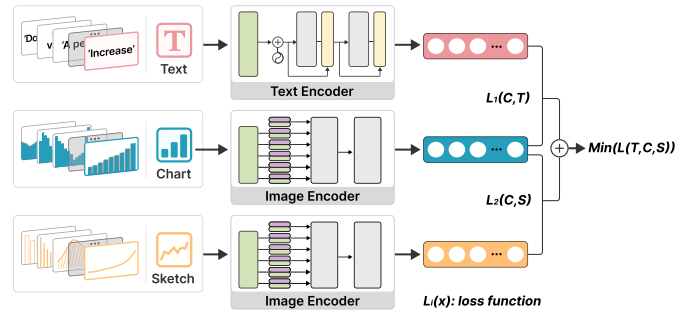


Fig. 4. The alignment pipeline for three modalities. Each modality is processed by a separate encoder, and the chart modality is set as the supervisor, guiding the alignment process.

Reference chart selection. Every user is given 100 real charts selected from our chart-text pairing dataset. The selected charts cover 23 categories of trend words, and contain bar, line, and area charts. 3) *Drawing.* The selected charts are displayed to the user one by one, and the user draws a sketch, which he/she thinks represents the change patterns in the displayed chart on the free-scale board. 4) *Evaluation/Redraw.* After drawing all the given charts, we show them the sketch with the corresponding chart one by one, and the user could delete or redraw the sketches they are not satisfied with. A total of 10 users (six women, four men) aged from 18 to 30 were invited. They all have knowledge of data visualization and are experienced in drawing sketches. In the end, we filter low-quality sketches, resulting in 1,214 pairs of chart-sketch pairings ready for training.

B. Modality Binding

We aim to bind all text \mathbb{T} , chart \mathbb{C} and sketch \mathbb{S} modalities together in a joint embedding space. Existing CLIP-based works predominantly focus on aligning pairs of modalities, while our objective is to accomplish the alignment of three modalities in the absence of the pairings between text and sketch modalities. As shown in Fig. 4, we employ a two-stage strategy: first, we employ modality-specific encoders to transform each modality into embeddings of uniform length [63]. All three modalities are processed using the Transformer architecture, leveraging its self-attention mechanism to effectively capture complex dependencies within each modality.

Given a chart C_i with its corresponding observation T_i in text modality, and observation S_i in sketch modality, we encode them into normalized embeddings: $p_i = f(C_i)$, $q_i = f(S_i)$, and $k_i = f(T_i)$, where f is a 63M-parameter 12-layer 512-wide Transformer with the architecture modifications with 8 attention heads [59] for text modality, and the Vision Transformer (ViT) [60] with a patch size of 32 for chart and sketch modalities. Each modality is processed by a separate encoder, which is designed to cater to the unique characteristics of the input. We add a modality-specific linear projection head on each encoder to obtain a fixed size d dimensional embedding, which is normalized, and set as p_i , q_i , and k_i for loss calculation. Besides facilitating learning, this setup allows us to initialize a subset of the encoders with weights from pre-trained CLIP [21] models. This initialization

not only provides a strong starting point for our MLLM but also enables it to better understand and align the semantic content across different modalities.

During the second stage, we combine the two-level cross-entropy and a bidirectional hinge-based triplet ranking loss to guide the three modalities to align in the latent space. We elect the chart modality, \mathbb{C} , as the supervised modality because visualization references are in the form of charts, and the chart-text and chart-sketch pairings that span a wide range of change patterns are well collected. Inspired by VSE++ [64], we address this by introducing the two-level cross-entropy and a bidirectional hinge-based triplet ranking loss, which makes the matched pairs have smaller entropies than unmatched ones. The formulation for the two cross-entropy functions is specified as:

$$H_1(C, T) = - \sum (p_i \times \log(k_i)), \quad (1)$$

$$H_2(C, S) = - \sum (p_i \times \log(q_i)), \quad (2)$$

where H_1 calculates the difference between charts C and text T , and (C, T) is the matched positive chart-text pair. H_2 calculates the difference between charts C and sketches S , and (C, S) is the matched positive chart-sketch pair.

We consider the loss function for the chart-text pairings as $L_1(C, T)$, and the loss function for the chart-sketch pairings as $L_2(C, S)$. Take chart and sketch modalities as an example, the loss is as follows:

$$L_2(C, S) = [\alpha + H_2(C', S) - H_2(C, S)]_+ + [\alpha + H_2(C, S') - H_2(C, S)]_+, \quad (3)$$

where α denotes the margin parameter, and $[x]_+ \equiv \max(x, 0)$. $C' = \arg \max_{X \neq C} H_2(X, S)$ and $S' = \arg \max_{Y \neq S} H_2(C, Y)$ denote the hardest negative corresponding to the positive pair (C, S) . The loss makes the chart embedding p_i and the sketch embedding q_i closer in the joint embedding space, and thus aligns \mathbb{C} and \mathbb{S} . Set L as the final loss of three modalities in the embedding space, that is, the sum of the two ranking losses: $L(T, C, S) = L_1(C, T) + L_2(C, S)$. By minimizing both the loss between chart and text modalities, and the loss between chart and sketch modalities, we achieve the alignment between the similar embeddings of the three modalities in a joint embedding space.

C. Implementation Details

We took a pre-trained CLIP text-image model and fine-tuned it on the selected chart-text and chart-sketch pairings. In the training phases, we employed a strategy where we froze the ViT encoder and conducted fine-tuning for 30 epochs with a batch size of 32, and a learning rate of $1e^{-5}$. The model parameters were optimized using AdamW optimizer, employing Betas (0.9, 0.98), weight decay of 0.001, and incorporating of StepLR learning rate schedule. This static scheduler ensures that the learning rate gradually decreases during fine-tuning, facilitating convergence towards a local optimum. Through using the modalities paired with charts, *i.e.*, pairs of the form (\mathbb{C}, \mathbb{T}) , and (\mathbb{C}, \mathbb{S}) to align each the embeddings from text modality \mathbb{T} and sketch modality \mathbb{S} to

those from charts. We observe that the pairs (T, S) are aligned even though we only train using the pairs (C, T) and (C, S) . This behavior is also validated by IMAGEBIND [45] so we reference to its statement that (\mathbb{C}, \mathbb{S}) and (\mathbb{C}, \mathbb{T}) are naturally aligned, and the text \mathbb{T} and sketch modalities \mathbb{S} constitute an emergency alignment.

V. VisTR SYSTEM

With the MLLM for multimodal visualization alignment, we build *VisTR* system that allows users to intuitively explore, comprehend, and interact with tabular data using visualizations as the *representation*. This section details the implementation of *visualization referencng* (Sect. V-A), *visualization pruning* (Sect. V-B), and *visualization interaction* (Sect. V-C) in *VisTR* system.

A. Visualization Referencing

This module is designed to ensure that the generated visualization references can effectively capture comprehensive data patterns inherent in the raw tabular data. To this end, we design a two-stage approach that first generates data facets to capture all underlying data change patterns and then maps all data facets into visualization references.

Facet Generation. In the first stage, we aim to capture meaningful data facets of the input table as comprehensively as possible. If we use violent enumeration, it will produce a lot of candidate data facets, and many of them will not include data trends. To avoid the inefficient data facet generation, we adopt the idea of subset embedding [33] indicating that patterns of multi-dimensional data are often related to subsets rather than records. Specifically, we adopt a multifaced process that incorporates a dual strategy of smoothing and segmentation.

Consider an input time-series table $D(timestamp, d_1, d_2, \dots, d_n)$, where each d_i represents a distinct variable containing a sequence of data points indexed by the timestamp. The first step is to smooth each variable d_i to retain essential patterns while filtering out the noise. To achieve this, *VisTR* employs Gaussian Smoothing, a technique favored for maintaining shape consistency under the Fourier transform [65]. Formally, for each each variable d_i , the smoothed series \tilde{d}_i is obtained as: $\tilde{d}_i = GaussianSmoothing(d_i)$. Compared with widely used Moving Average (MA) or Weighted Moving Average (WMA) [66], Gaussian Smoothing can not only preserve key features while smoothing but also have flexibility in parameter control.

After smoothing, we segment each smoothed variable \tilde{d}_i into distinct facets to extract meaningful and reliable patterns. The segmentation process is defined as $R(\tilde{d}_i) = \{r_1(\tilde{d}_i), r_2(\tilde{d}_i), \dots, r_m(\tilde{d}_i)\}$, where $r_j(\tilde{d}_i)$ represents a subset (termed as a facet) of \tilde{d}_i . To ensure each data facet reflects a valid data pattern, we incorporate the Page-Hinckley Test (PHT) [67] to detect critical points where shifts occur, thereby delineating the boundaries between different facets. Specifically, the segmentation process can be formalized as $R(\tilde{d}_i) = PHT(\tilde{d}_i)$. Additionally, we aggregate continuous subsets to form new facets, enabling the inclusion of segments with varying lengths.

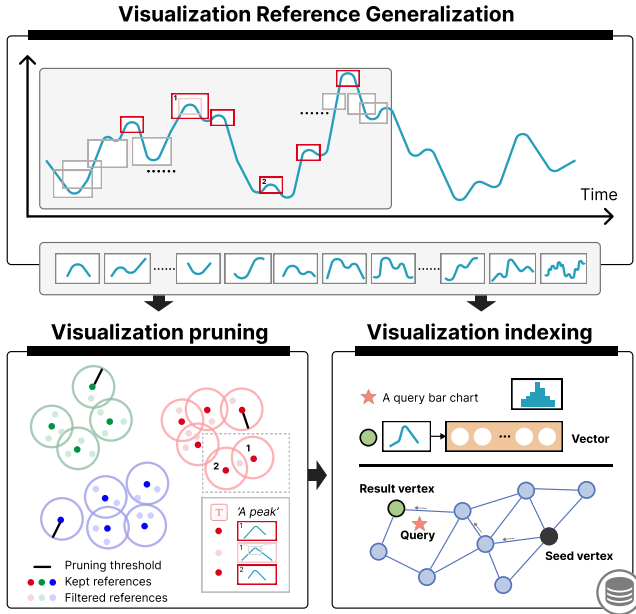


Fig. 5. The pipeline of *visualization referencing* and *visualization pruning* modules. Visualization pruning and indexing are used to accelerate the storage and retrieval process.

Visual Mapping. The second stage is visual mapping, where we transform each data facet into a standard visual representation. This process leverages the *matplotlib* library to generate fixed-size visualization references devoid of axes, specifically utilizing bar, line, and area charts to manifest the trend within each data facet. The uniformity provided by fixed-size visualization references improves the fine-tuned MLLM’s capacity to analyze and process them. For each data facet $r_j(\tilde{d}_i) \in R(\tilde{d}_i)$, the visual mapping process transforms $r_j(\tilde{d}_i)$ into a fixed-size visualization reference c_j , which is formalized as $c_j = vmap(r_j(\tilde{d}_i))$. The collection of all visualization references derived from the data facets of a particular variable d_i is represented as $C(d_i) = \{c_1, c_2, \dots, c_m\}$. Collectively, for all variables in the input table D , the visualization references are denoted as $C = \bigcup_{i=1}^n C(d_i) = \{c_{i,j} | d_i \in D, r_j(d_i) \in R(d_i)\}$.

B. Visualization Pruning and Indexing

For a given table, we will generate a vast collection of visualization references, each of which is subsequently mapped into vector representations (*i.e.*, embeddings). The large number of visualization references poses significant challenges to efficient storage and retrieval. To address these challenges, we design a combined approach of visualization pruning and indexing, as illustrated in Fig. 5, to improve *VisTR*’s ability to manage and retrieve visualization references.

Visualization Pruning. Here, the key idea is to filter out less informative visualization references in advance while retaining those that provide significant insights. The main challenge lies in discerning and preserving highly valuable visualization references during pruning. For all visualization references for a variable d_i , it may encounter a scenario where two references exhibit similar change patterns, and one is entirely encompassed by the other. We quantify the similarity between visualization vectors using the Euclidean distance $d(c_j, c_k)$

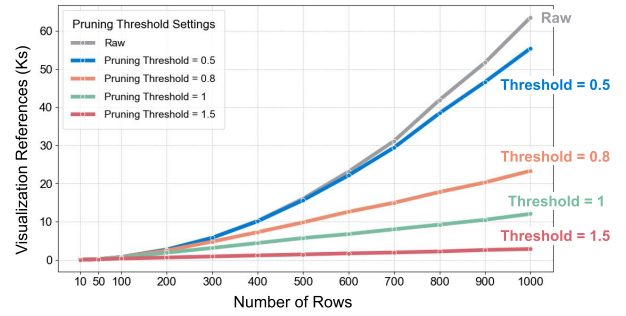


Fig. 6. The relationship between the number of visualization references, table rows, and the pruning threshold. The remaining visualization references are close to approximately 20% of the raw number when the pruning threshold is set to 1.

between the two vectors c_j and c_k . We introduce a pruning threshold to determine whether two visualization vectors are sufficiently similar to warrant pruning. If $d(c_j, c_k)$ is less than the set pruning threshold, the vector covering a shorter time range is filtered out. An example scenario is illustrated in Fig. 5, where the ‘a peak’ change pattern exists in pink-boxed visualization references. In this case, the light-pink-boxed one has less information and is consequently filtered out.

The pruning threshold acts as a predefined parameter that affects the number of stored visualization references. To assess its impact, we designed an experiment with four values: 0.5, 0.8, 1, and 1.5, and applied the thresholds to tables of varying row counts. Specifically, the row numbers were considered based on the typical sizes used in existing LLM-based table reasoning methods, which typically support data tables with fewer than 50 rows. For instance, Tabfact [68], a commonly used dataset containing over 16k Wiki tables, has an average of 12.96 rows per table (max.=48, min.=1, std.=8.46). Given the focus on time-series data tables and long-term trend analysis, we extended the experiment to tables with up to 1000 rows, approximately encompassing four trading years. We calculated the average number of visualization references across three sub-tables with corresponding table sizes extracted from the DJI. data table for each pruning threshold.

Fig. 6 shows the relationship between the number of stored visualization references, the number of data table rows, and the pruning thresholds. When the pruning threshold is set to 1, the number of stored visualization references approximated 20% of the raw reference number. This aligns with the well-known Pareto principle (80/20 rule) [69], which is widely leveraged in various optimization strategies to balance efficiency and information retention. As such, we also set the pruning threshold to be 1. This strikes a balance between maintaining a rich representation set and reducing the storage footprint.

Visualization Indexing. For efficient retrieval of visualization references, we utilize an open-sourced vector database named Chroma [56], which enables effective indexing and retrieval of embeddings. Specifically, we first apply our fine-tuned MLLM to encode all visualization references into 512-dimensional vectors. Chroma automatically maintains an index document when encoding all visualization references for retrieval. These indexes compress vectors into codes of a fixed size, storing them in an array. For similarity measurement, we employ the dot product function. By leveraging Chroma’s advanced

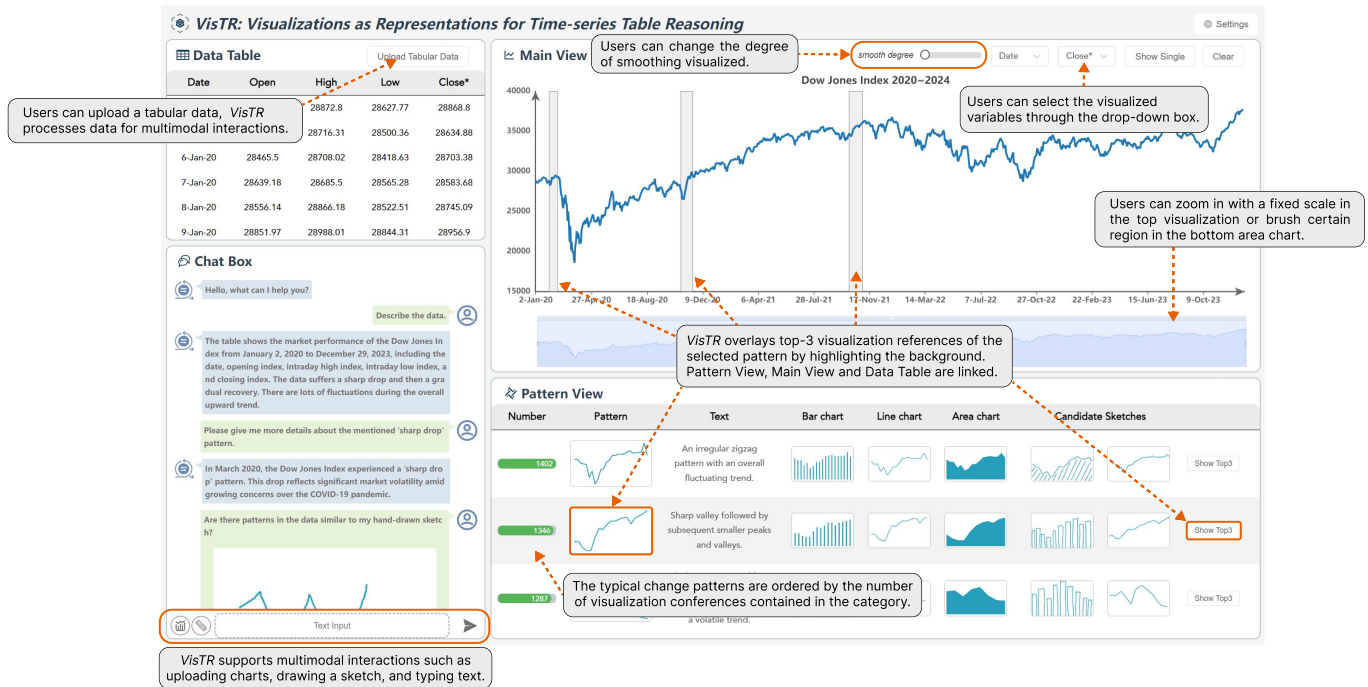


Fig. 7. The interactive interface of VisTR, which contains four main views and supports multimodal interactions for table reasoning.

indexing capabilities, VisTR efficiently speeds up the retrieval process to handle vast amounts of visualizations, ensuring both speed and accuracy.

C. Visualization Interaction

The Decomposing-Execution-Filling Strategy. Inspired by Dater [13], we introduce a ‘decomposing-execution-filling’ strategy to decompose and parse multimodal user queries and return results that meet user expectations. Specifically, we first decompose a user’s table reasoning queries and convert them into visualization reference retrieval operations, similar to text-to-SQL parsing (e.g., [30], [70]). Afterward, we execute the visualization retrieval operations in Chroma and get the result for back-filling the final response.

Here, we employ two LLMs with in-context learning using prompts to decompose user queries and complete outputs respectively. Below we illustrate an example using the case shown in Fig. 1(A). Given the query “What is the price trend of Apple during March?”, we first decompose the question into a retrieval task “return the visualization reference of Apple price in March”, and a cross-modal alignment task “recognize the trend in the retrieved visualization reference”. The corresponding visualization reference is first retrieved from Chroma, and then aligned with the ‘two peaks’ pattern to generate the final textual response “There is a two-peak price trend in Apple during March.”. Detailed prompts are provided in our open-sourced code.

Visual Interface. In addition to textual responses, VisTR also incorporates a user-friendly interface to enable intuitive table reasoning and exploration. As shown in Fig. 7, the interface includes four main views: (A) Data Table, (B) Main View, (C) Chat Box, and (D) Pattern View. When a user uploads a table, the back-end of VisTR processes the tabular data into

visualization references and stores them in the vector database, while the front-end interface displays the uploaded table in Data Table, and presents the visualization for the data in the Main View. By default, Main View uses an area graph for the overall context information and a line chart for the details. Various operations, such as selecting different variables or combinations of variables to display, are enabled in the drop-down box in the upper right corner of Main View. For the display of multi-variables, we use a multi-line chart with colors to encode different variables. The bottom area chart also allows for fixed-scale zooming and brushing, allowing users to observe detailed variable changes.

The Chat Box provides a dialogue window that supports multi-round conversations and multimodal inputs including uploading charts, drawing sketches, and typing text. Textual responses to user queries are also displayed in the Chat Box. The responses are also connected to Main View, where the corresponding visualization reference is highlighted. Pattern View presents groups of typical data change patterns for the variable selected in Main View. These groups are ordered from top to bottom, with the most populated data change pattern at the top, tapering to the least at the bottom. Users can select a specific group of data change patterns, and then the top-3 visualization references of this pattern will be overlaid by highlighting the background. If there is an overlap among the displayed visualization references, the overlapping area corresponds to a darker background color. For users wishing to delve into each reference in detail, users can click the ‘show’ button located in the upper right corner of the Main View to achieve a circular review of each one. Additionally, Pattern View provides multimodal information (descriptive text, different chart types, and candidate sketches) for a single variable’s typical change patterns, including descriptive text, various charts, and potential sketch candidates.

VI. EVALUATION

To thoroughly evaluate *VisTR*, we conduct both quantitative evaluations and case studies. In the quantitative evaluations (Sect. VI-A), we assess the alignment ability of our fine-tuned MLLM. Subsequently, we present two classic cases on actual application scenarios (Sects. VI-B & VI-C), representing a possible pathway through multimodal interactions to complete a time-series table reasoning task.

A. Effectiveness of Multimodal Visualization Alignment

We evaluate the alignment performance of our multimodal visualization alignment model from two perspectives: quantitative evaluation on text-chart retrieval, and user recognition on sketch-chart retrieval.

1) *Baselines and Metrics*: We compare our fine-tuned MLLM against several pre-trained models: CLIP [21], OpenCLIP [71], and UniChart [36]. Our MLLM is a fine-tuned CLIP model on the composite dataset. To highlight the necessity and impact of the fine-tuning process, we compare it with the zero-shot CLIP and OpenCLIP models as an ablation study. Additionally, we validate the effectiveness of our fine-tuned CLIP by comparing it against OpenCLIP and UniChart, confirming the appropriateness of our model selection. *VisTR* enables comprehensive multimodal binding among different modalities, rather than performing direct subsequence or sketch matching. In this sense, we omit the comparison with existing sketch query [41], [72] or sequence matching systems [73], [74].

Considering the imbalance among different trend word categories, we set two metrics for a comprehensive evaluation:

- **Top-1 Accuracy (Acc)**. The accuracy calculates the ratio of true accurately identified pairs to the total number of pairs examined.
- **Weighted F1-Score (WF)**. WF adopts the weighted average considering the unevenness of the categories, which is calculated as: $WF = \frac{1}{T_N} \sum_{i=1}^{T_N} \frac{2 \times P_i \times R_i}{(P_i + R_i)}$, where R_i and P_i are the recall and precision of the i^{th} trend-word category, respectively.

2) *Text-Chart Retrieval*: To rigorously assess the performance of our fine-tuned visualization alignment model in aligning chart-text pairs, we ensure that the evaluation dataset includes chart types of bar, line, and area chart, as well as all $T_N = 23$ categories of trend words. Specifically, we randomly select 20% of the data for each chart type and each trend category from the chart-text pairing dataset for evaluation.

Results. The quantitative results are presented in Table. I. Our fine-tuned MLLM demonstrates robust performance in aligning chart and text modalities, with overall accuracy and weighted F1-score exceeding 85% across all chart types. The results for each individual chart type also provide substantial evidence of the model’s effectiveness across various chart types. However, we observed that bar charts yield slightly lower metrics than other chart types. This discrepancy may be attributed to the inherent characteristics of bar charts, which utilize separated bars to encode data, resulting in less distinctiveness compared to the continuous line marks used in

TABLE I
EXPERIMENTAL RESULTS ON CHART-TO-TEXT RETRIEVAL TEST FOR ALL AND INDIVIDUAL CHART TYPES.

Model		All	Bar	Line	Area
Ours (Fine-tuned CLIP)	Acc (%)	89.02	86.29	89.00	89.12
	WF (%)	87.45	85.91	86.54	87.79
Fine-tuned OpenCLIP	Acc (%)	50.74	50.36	51.86	50.24
	WF (%)	49.77	48.04	46.41	49.73
Zero-shot CLIP	Acc (%)	0.82	1.10	0.72	1.02
	WF (%)	0.36	0.29	0.11	0.07
Zero-shot OpenCLIP	Acc (%)	7.71	8.20	5.27	1.08
	WF (%)	5.37	3.78	1.95	0.30



Fig. 8. Ratings of the visual similarity between pairs of the matched sketches and charts across our fine-tuned MLLM and three pre-trained models based on a 5-point Likert scale.

line charts and the filled area marks used in area charts. To enhance the accuracy of bar charts, factors such as bar widths may need to be considered during fine-tuning process.

The comparisons between fine-tuned CLIP and zero-shot CLIP models confirm that fine-tuning is crucial for enhancing model performance in our specific domain. While zero-shot OpenCLIP slightly outperforms zero-shot CLIP, fine-tuned CLIP significantly surpasses fine-tuned OpenCLIP. Zero-shot OpenCLIP outperforms zero-shot CLIP is probably due to more extensive pre-training data that include more diverse chart images. However, after fine-tuning, CLIP’s architecture process is better suited for our specific requirements. Its superior results validate our choice of CLIP as the base model.

3) *Sketch-Chart Retrieval*: We validate the alignment for chart-sketch pairs through a user study. Initially, we randomly selected 200 sketches from the chart-sketch dataset. Then, we tasked each of the four models (ours, CLIP, OpenCLIP, and UniChart) with determining the closest chart in the intent space to each selected sketch, indicating the chart with the highest similarity. This process constructed 800 matched sketch-chart pairings for the subsequent user study. We recruited 30 participants (15 women, and 15 men) with experience in building charts. Each participant is randomly given 20 sketches with their matched charts by each model and asked to rate the similarity between pairs of matched sketches and charts for each model, based on their visual perception of the correspondences. The ratings are gathered using a 5-point Likert scale [75], which provides a quantitative measure of the user agreement or disagreement with the similarities of chart-sketch pairs.

As shown in Fig. 8, our model achieved the highest similarity agreement among participants (Mean = 4.33, SD = 0.67), and the Unichart achieved the lowest agreement with Mean = 2.25 and SD = 1.17. Given the non-normal distribution of collected ratings, we initiated our analysis by conducting the *Friedman test* to evaluate the statistical significance of ratings among the four models. The p-value of the *Friedman test* is less than 0.01, indicating significant differences between

models. To further pinpoint the specific differences among models, we employed the *Wilcoxon signed-rank test* for paired comparisons, accompanied by *Bonferroni correction* to control errors. The pairwise comparisons showed that our model significantly outperformed the others, as detailed in Fig. 8. The poor performance of UniChart may be due to its focus on OCR features rather than chart features, leading to a weaker grasp of the varied patterns present within charts and hand-drawn sketches. The comparison results underscore the importance of encoding patterns in our alignment model, confirm the judicious choice of CLIP-ViT as our base pre-trained model, and highlight the superiority of our fine-tuned model in binding sketch and chart modalities.

B. Case Study 1: Financial Data Exploration

In this case, we consider a financial data exploration scenario. A market analyst, Mike, is studying the Dow Jones Index (DJI.)’s change patterns post-COVID-19. The used data measures the daily price movements of 30 large US companies, spanning from January 2nd, 2020 to December 29th, 2023. The data includes five columns: Date, Open, High, Low, and Close, detailing the trading metrics for each business day. Mike first loads the DJI. data into *VisTR* and selects ‘Close’ as the displayed variable in the Main View. *VisTR* initially generates 64,261 visualization references, among which 13,823 visualizations are pruned for exploration. The average retrieval time for querying a visualization reference stored in Chroma is within 0.6s.

As shown in Fig. 9, Mike explores the data as follows.

- **Table Summarization.** Mike first enters the dialogue box “Describe the data.”. The response from *VisTR* includes two parts, one is the basic table description “The table shows the market performance of the Dow Jones Index from January 2, 2020, to December 29, 2023, including the date, opening index, intraday high index, intraday low index, and closing index.”, and the other is the overall trend description “The data suffers a sharp drop and then a gradual recovery. There are lots of fluctuations during the overall upward trend.”.
- **Question & Answering.** Given this description, Mike is interested in the “sharp drop” pattern, so he tries to locate the pattern by entering the text “Please give me more details about the mentioned ‘sharp drop’ pattern.”. Based on the context, *VisTR* can easily locate the “sharp drop” pattern that appears, and the matched interval is highlighted in Main View. At the same time, a text description “In March 2020, the Dow Jones Index experienced a ‘sharp drop’ pattern. This drop reflects significant market volatility amid growing concerns over the COVID-19 pandemic.” is returned in the dialogue box.
- **Visual Query.** Mike then freely sketches a ‘w’ pattern  in the empty canvas and enters “Are there patterns in the data similar to my hand-drawn sketch?”. *VisTR* retrievals for the visualization references similar to the input hand-drawn sketch from the vector database, and returns the three most similar matches in Main View. To facilitate user understanding, *VisTR* also returns a text description

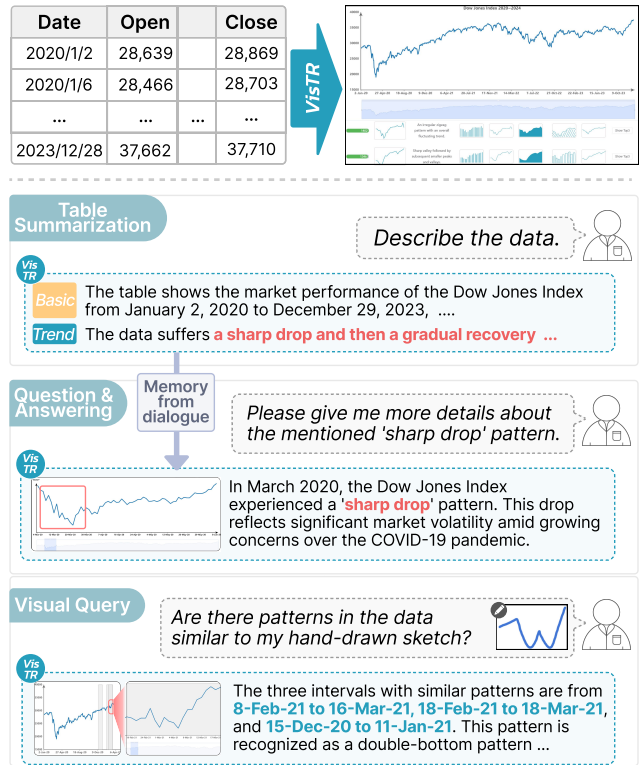


Fig. 9. Case study 1: data exploration for DJI. form 2020 to 2023. Mike gets a complete understanding of the data via table summarization, question & answering, and visual query enabled by *VisTR*.

of the matched results: “The three intervals with similar patterns are from 8-Feb-21 to 16-Mar-21, 18-Feb-21 to 18-Mar-21, and 15-Dec-20 to 11-Jan-21. This pattern is recognized as a double-bottom pattern. It occurred in December 2020 and February 2021 suggesting that during both periods, the market demonstrated buyer interest at lower price levels after experiencing declines. This support prevented further downward movement. Higher prices prompted more buyers to participate, contributing to the Dow’s upward momentum.”.

In this way, Mike gets an overall understanding of the tabular data, and also typical trends and patterns within the data. The multimodal interactions, together with visual interactions like selecting and zooming in the visual interface, enable Mike to easily understand the DJI. data and recognize interesting data change patterns.

C. Case Study 2: Air Pollutant Analysis

In the second case, we demonstrate the workflow of mining relationships between data change patterns of different variables. A student, Emily, is seeking the correlations between different air pollutants. The used air pollutant dataset includes the daily air quality metrics from January 1, 2017, to December 31, 2018, which is collected by the Beijing US Embassy¹. The data includes variables of Date, PM25, O3, temperature, and relative humidity, which provides insights into the fluctuations in air quality and correlations between air pollutants. Emily first loads the pollutant data into *VisTR*,

¹<https://aqicn.org/city/beijing/us-embassy/cn/>

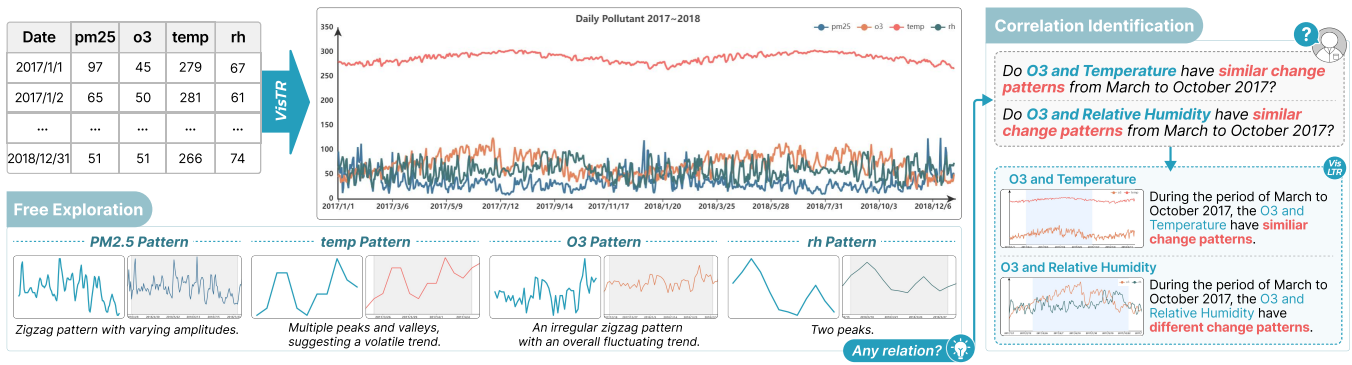


Fig. 10. Case study 2: multivariate analysis for the uploaded air pollutant dataset. With *VisTR*, Emily recognizes typical data change patterns and relationships between different air pollutants.

which generates a multi-line chart with each line representing a variable. In the backend, *VisTR* generates a total of 102,787 visualization references, of which 40,243 are stored in Chroma after pruning.

Fig. 10 illustrates Emily’s analysis process using *VisTR* to explore the multivariate data.

- **Free Exploration.** To obtain the typical data change patterns of pollutants, Emily selects four pollutant indicators, *PM25*, *O3*, *temperature*, and *relative humidity*, and obtains the change patterns in the Pattern View. She notices that all four indicators exhibit obvious daily fluctuations. Specifically, *PM25* exhibits a ‘zigzag pattern with varying amplitudes.’, indicative of its dynamic nature and daily variability. Similarly, a typical pattern of *O3* is ‘An irregular zigzag pattern with an overall fluctuating trend.’, further highlighting the pronounced daily jitters in pollutant levels. These observations motivate Emily to explore the relationship between these pollutant indicators over a long time interval.
- **Correlation Identification.** Different indicators have different data ranges, making it difficult to directly observe the relationships between different indicators in the Main View. For instance, the value of temperature is always greater than 250 (K), while the value of *O3* hovers around 50 ($\mu\text{g m}^{-3}$). To examine the correlation of these indicators, Emily chooses to directly raise questions to *VisTR* in the Chat Box. She enters “Do *O3* and temperature have similar change patterns from March to October 2017?”. The *O3* and temperature data change patterns during this period are highlighted in Main View and the response by *VisTR* is returned in the dialogue box: “During the period of March to October 2017, the *O3* and Temperature have similar change patterns.”, and the response indicates a similar pattern between the indicators during the period. Emily further asks about the relationship between *O3* and relative humidity, by entering “Do *O3* and Relative Humidity have similar change patterns from March to October 2017?”. From the response, Emily can understand the data change patterns of *O3* and relative humidity are different.

In this manner, Emily gains a comprehensive insight into the multivariate air pollutant data, recognizing both the typical data change patterns and correlations among various air

pollutant indicators.

VII. DISCUSSION

The case studies have demonstrated *VisTR*’s capability in recognizing and explaining data change patterns within tabular data. By leveraging visualizations as representation, *VisTR* successfully addresses the limitations of existing LLM-based table reasoning methods in pattern recognition and visual-based pattern exploration. Moreover, the process also aligns with the exploratory data analysis (EDA) process. EDA often involves summarizing the main characteristics of a dataset using visualization, enabling users to understand the data’s structure, recognize patterns, detect anomalies, and formulate hypotheses for further investigation. In this sense, the proposed framework not only streamlines the process of EDA but also expands its horizons, providing users with novel approaches to uncover hidden patterns within datasets.

Generalizability. Nevertheless, to fully realize the potential of the proposed framework, we need to enhance the generalizability of *VisTR* from the following perspectives.

- **More table types.** *VisTR* is currently instantiated on time-series tables, which contain data change patterns that cannot be processed by existing SQL-based LLMs for table reasoning. *VisTR* has the potential to be extended to more general table types by employing alternative data transformation methods within the *visualization referencing* module. For instance, *VisTR* can be adapted to recognize and analyze the distribution patterns in a student grade table. In this scenario, a data aggregation method could be employed to recognize grade distribution patterns, such as the normal distribution. Supporting a broader range of table types is feasible, leveraging methods such as subset embedding [33] and learning-based approaches [34].
- **General queries.** *VisTR* focuses on tasks related to reasoning about data change patterns in tables. Therefore, we primarily provide text-based user queries related to data change patterns, such as “what type of change pattern exists in the data?” However, this narrow focus also limits our ability to handle other general user queries, including those related to causal reasoning, such as “why did Apple stock rise in March?” When posed with such questions, *VisTR* may encounter the ‘hallucination’ issue, leading

to incorrect queries and responses. To achieve a comprehensive exploration and reasoning of a data table, we require more general user queries, which may necessitate the incorporation of external knowledge sources.

- *Dataset bias.* The successful alignment of our model heavily relies on acquiring high-quality training data. However, the dataset used for fine-tuning, while demonstrating its effectiveness, is limited in size and diversity, posing challenges to generalizability. This limitation becomes particularly evident when handling complex or unconventional sketch representations, where a richer and more diverse dataset is essential for robust model fine-tuning. The dataset collection process itself introduces potential biases and inconsistencies. Scaling up the dataset to address these limitations presents significant challenges. First, the limited number of users contributing to user-labeled sketches may embed subjective preferences into the chart-sketch-text pairings. While crowdsourcing strategies offer a way to accelerate data collection, they are prone to similar subjective biases and the quality control for such large-scale manual efforts remains a significant challenge. An innovative alternative lies in data augmentation techniques to reduce reliance on manual sketch collection. Second, the filtered trend words from textual descriptions may oversimplify visual information, neglecting nuances in semantics. To enrich textual descriptions, a potential solution proposed by Time-LLM [76] is to generate text prototypes by assembling candidate vocabularies. Then the generated rich text descriptions can be paired with charts through crowd-sourced rating frameworks [77].
- *Intent-enhanced sketches.* Users' intuition about sketching targets often emerges from the exploration process. As a reason, *VisTR* offers insights into common patterns within the uploaded table. However, expressing complex or uncommon patterns solely through hand-drawn sketches can be challenging for users [22]. To address this challenge, several solutions can be considered. First, incorporating additional interactive features like dragging, resizing, and erasing can provide users with greater flexibility in adjusting their intent [78]. Summarizing multi-attribute temporal patterns and introducing a more effective time-series segmentation method have shown promise in addressing this issue [79]. By implementing these methods, we can further enhance the capabilities of *VisTR* to support sketches with enhanced intents.

VisTR vs. Traditional Methods. *VisTR* introduces an innovative attempt to convert time-series tables into visual representations, enabling efficient multi-modal binding and continuous context reasoning. Compared to traditional subsequence or sketch matching methods, such as metric-based [41], regular expression-based [74] or deep-learning-based approaches [72], *VisTR* processes varying data facet lengths into uniform vision tokens, offering smoother multi-modal interaction and significant resource savings due to reduced prompt lengths [80]. However, visual representations come with notable limitations. They often underperform traditional metric-based methods in

matching precision, incur higher storage costs, and may ignore shorter time subsequences in *visualization referencing* module. Additionally, fine-tuning models for aligning modalities of chart, sketch, and text is resource-intensive. Despite these challenges, the rapid advancements of multi-modal large language models (MLLMs) make this research direction promising. Future efforts should focus on improving precision and optimizing storage efficiency to fully leverage the potential of visual representations in advancing multi-modal frameworks.

Potential scenarios. Besides table reasoning, the proposed framework holds potential for other application scenarios, such as safeguarding sensitive data that requires a balance between data privacy and utility. By transforming raw tabular data into visualizations, *VisTR* shields the secure information contained within tables from users, while still allowing for examination and querying of the data patterns. Moreover, *VisTR* could also find applications in fraud detection, as visualizations generated from transactional data could help recognize suspicious patterns indicative of fraudulent activities.

VIII. CONCLUSION

We present *VisTR*, a new framework for time-series table reasoning that leverages visualizations as *representations* to bridge raw data and human cognition. By enabling enhanced pattern recognition, mitigating context drift, and supporting visual-based exploration, *VisTR* addresses key limitations of existing LLM-based methods. *VisTR* integrates a fine-tuned MLLM, trained on a newly constructed dataset of chart-text and chart-sketch pairs, to align charts, text, and sketches in a unified embedding space. Combined with strategies for visualization referencing, pruning, and indexing, *VisTR* provides an interactive system for seamless multimodal interactions with time-series tables. Quantitative evaluations and case studies demonstrate its effectiveness in aligning multimodal inputs and improving reasoning accuracy. *VisTR* opens new research directions for integrating visualizations into table reasoning and enhancing multimodal data exploration. Future work will extend its applicability to broader table types, generalized queries, and diverse application scenarios.

REFERENCES

- [1] J. Hao, M. Yang, Q. Shi, Y. Jiang, G. Zhang, and W. Zeng, "Finflir: Automating graphical overlays for financial visualizations with knowledge-grounding large language model," *IEEE Trans. Vis. Comput. Graph.*, pp. 1–17, 2024.
- [2] C. Chai, J. Wang, Y. Luo, Z. Niu, and G. Li, "Data management for machine learning: A survey," *IEEE Trans. Knowl. Data Eng.*, vol. 35, no. 5, pp. 4646–4667, 2023.
- [3] J. Lin, S. Williamson, K. Borne, and D. DeBarr, "Pattern recognition in time series," *Advances in Machine Learning and Data Mining for Astronomy*, vol. 1, no. 617–645, p. 3, 2012.
- [4] Y. Chen, M. A. Nascimento, B. C. Ooi, and A. K. Tung, "Spade: On shape-based pattern detection in streaming time series," in *Proc. IEEE ICDE*. IEEE, 2006, pp. 786–795.
- [5] Y. Ye, J. Hao, Y. Hou, Z. Wang, S. Xiao, Y. Luo, and W. Zeng, "Generative AI for visualization: State of the art and future directions," *Vis. Informatics*, vol. 8, no. 1, pp. 43–66, 2024.
- [6] B. Li, Y. Luo, C. Chai, G. Li, and N. Tang, "The dawn of natural language to SQL: are we fully ready?" *Proc. VLDB Endow.*, vol. 17, no. 11, pp. 3318–3331, 2024.

- [7] X. Liu, S. Shen, B. Li, P. Ma, R. Jiang, Y. Luo, Y. Zhang, J. Fan, G. Li, and N. Tang, "A survey of NL2SQL with large language models: Where are we, and where are we going?" *CoRR*, vol. abs/2408.05109, 2024.
- [8] J. Zhang, J. Xiang, Z. Yu, F. Teng, X. Chen, J. Chen, M. Zhuge, X. Cheng, S. Hong, J. Wang, B. Zheng, B. Liu, Y. Luo, and C. Wu, "Aflow: Automating agentic workflow generation," *CoRR*, vol. abs/2410.10762, 2024.
- [9] W. Chen, "Large Language Models are few(1)-shot Table Reasoners," in *Proc. EACL*, 2023, pp. 1090–1100.
- [10] Z. Zhang, Y. Wu, Y. Luo, and N. Tang, "MAR: matching-augmented reasoning for enhancing visual-based entity question answering," in *EMNLP*. Association for Computational Linguistics, 2024, pp. 1520–1530.
- [11] Z. Wang, H. Zhang, C. Li, J. M. Eisenschlos, V. Perot, Z. Wang, L. Miculicich, Y. Fujii, J. Shang, C. Lee, and T. Pfister, "Chain-of-Table: Evolving Tables in the Reasoning Chain for Table Understanding," in *Proc. ICLR*, 2024.
- [12] X. Zhang, D. Wang, L. Dou, B. Wang, D. Wu, Q. Zhu, and W. Che, "FLEXTAF: Enhancing Table Reasoning with Flexible Tabular Formats," *arXiv preprint arXiv:2408.08841*, 2024.
- [13] Y. Ye, B. Hui, M. Yang, B. Li, F. Huang, and Y. Li, "Large language models are versatile decomposers: Decomposing evidence and questions for table-based reasoning," in *Proc. ACM SIGIR*, 2023, pp. 174–184.
- [14] Z. Cheng, T. Xie, P. Shi, C. Li, R. Nadkarni, Y. Hu, C. Xiong, D. Radev, M. Ostendorf, L. Zettlemoyer, N. A. Smith, and T. Yu, "Binding Language Models in Symbolic Languages," in *Proc. ICLR*, 2023.
- [15] L. Gao, A. Madaan, S. Zhou, U. Alon, P. Liu, Y. Yang, J. Callan, and G. Neubig, "PAL: Program-aided Language Models," in *Proc. IEEE ICML*, vol. 202, 2023, pp. 10764–10799.
- [16] H. Kim, B.-H. So, W.-S. Han, and H. Lee, "Natural language to SQL: Where are we today?" *Proc. VLDB*, vol. 13, no. 10, pp. 1737–1750, jun 2020.
- [17] L. Chen, M. Zaharia, and J. Zou, "How is ChatGPT's Behavior Changing over Time?" *arXiv preprint arXiv:2307.09009*, 2023.
- [18] Y. Zhu, S. Du, B. Li, Y. Luo, and N. Tang, "Are large language models good statisticians?" *CoRR*, vol. abs/2406.07815, 2024.
- [19] Y. Wu, L. Yan, L. Shen, Y. Wang, N. Tang, and Y. Luo, "Chartinsights: Evaluating multimodal large language models for low-level chart question answering," in *EMNLP (Findings)*. Association for Computational Linguistics, 2024, pp. 12174–12200.
- [20] G. Li, R. Li, Y. Feng, Y. Zhang, Y. Luo, and C. H. Liu, "Coinsight: Visual storytelling for hierarchical tables with connected insights," *IEEE Trans. Vis. Comput. Graph.*, vol. 30, no. 6, pp. 3049–3061, 2024.
- [21] A. Radford, J. W. Kim, C. Hallacy, A. Ramesh, G. Goh, S. Agarwal, G. Sastry, A. Askell, P. Mishkin, J. Clark, G. Krueger, and I. Sutskever, "Learning Transferable Visual Models From Natural Language Supervision," in *Proc. IEEE ICML*, vol. 139, 2021, pp. 8748–8763.
- [22] D. J.-L. Lee, J. Lee, T. Siddiqui, J. Kim, K. Karahalios, and A. Parameswaran, "You can't always sketch what you want: Understanding Sensemaking in Visual Query Systems," *IEEE Trans. Vis. Comput. Graph.*, vol. 26, no. 1, 2020.
- [23] W. Chen, H. Wang, J. Chen, Y. Zhang, H. Wang, S. Li, X. Zhou, and W. Y. Wang, "TabFact: A Large-scale Dataset for Table-based Fact Verification," in *Proc. ICLR*, 2020.
- [24] N. Jin, J. Siebert, D. Li, and Q. Chen, "A Survey on Table Question Answering: Recent Advances," in *Proc. CCKS*, vol. 1669, 2022, pp. 174–186.
- [25] J. M. Eisenschlos, S. Krichene, and T. Müller, "Understanding tables with intermediate pre-training," in *Proc. EMNLP*, vol. EMNLP 2020, 2020, pp. 281–296.
- [26] Q. Liu, B. Chen, J. Guo, M. Ziyadi, Z. Lin, W. Chen, and J. Lou, "TAPEX: Table Pre-training via Learning a Neural SQL Executor," in *Proc. ICLR*, 2022.
- [27] Z. Jiang, Y. Mao, P. He, G. Neubig, and W. Chen, "OmniTab: Pretraining with natural and synthetic data for few-shot table-based question answering," *arXiv preprint arXiv:2207.03637*, 2022.
- [28] T. Kojima, S. S. Gu, M. Reid, Y. Matsuo, and Y. Iwasawa, "Large Language Models are Zero-Shot Reasoners," in *Proc. NeurIPS*, 2022.
- [29] Y. Ye, B. Hui, M. Yang, B. Li, F. Huang, and Y. Li, "Large Language Models are Versatile Decomposers: Decomposing Evidence and Questions for Table-based Reasoning," in *Proc. ACM SIGIR*, 2023, pp. 174–184.
- [30] L. Wang, B. Qin, B. Hui, B. Li, M. Yang, B. Wang, B. Li, J. Sun, F. Huang, L. Si *et al.*, "PROTON: Probing Schema Linking Information from Pre-trained Language Models for Text-to-SQL Parsing," in *Proc. ACM KDD*, 2022, pp. 1889–1898.
- [31] S. Few, "Show me the numbers," *Analytics Pres*, 2004.
- [32] A. Lazard and L. Atkinson, "Putting environmental infographics center stage: The role of visuals at the elaboration likelihood model's critical point of persuasion," *Science Communication*, vol. 37, no. 1, pp. 6–33, 2015.
- [33] P. Xie, W. Tao, J. Li, W. Huang, and S. Chen, "Exploring Multi-dimensional Data via Subset embedding," *Comput. Graph. Forum*, vol. 40, no. 3, pp. 75–86, 2021.
- [34] Y. Sun, J. Li, S. Chen, G. Andrienko, N. Andrienko, and K. Zhang, "A learning-based approach for efficient visualization construction," *Visual Informatics*, vol. 6, no. 1, pp. 14–25, 2022.
- [35] A. Masry, X. L. Do, J. Q. Tan, S. Joty, and E. Hoque, "ChartQA: A Benchmark for Question Answering about Charts with Visual and Logical Reasoning," in *Proc. ACL*, 2022, pp. 2263–2279.
- [36] A. Masry, P. Kavehzadeh, X. L. Do, E. Hoque, and S. Joty, "Unichart: A Universal Vision-language Pretrained Model for Chart Comprehension and Reasoning," *arXiv preprint arXiv:2305.14761*, 2023.
- [37] E. Hoque, P. Kavehzadeh, and A. Masry, "Chart Question Answering: State of the art and future directions," *Comput. Graph. Forum*, vol. 41, no. 3, pp. 555–572, 2022.
- [38] S. Xiao, Y. Hou, C. Jin, and W. Zeng, "WYTIWYR: A User Intent-Aware Framework with Multi-modal Inputs for Visualization Retrieval," *Comput. Graph. Forum*, vol. 42, no. 3, pp. 311–322, 2023.
- [39] V. Schetinger, S. Di Bartolomeo, M. El-Assady, A. McNutt, M. Miller, J. P. A. Passos, and J. L. Adams, "Doom or Deliciousness: Challenges and Opportunities for Visualization in the Age of Generative Models," *Comput. Graph. Forum*, vol. 42, no. 3, pp. 423–435, 2023.
- [40] S. Xiao, S. Huang, Y. LIN, Y. Ye, and W. Zeng, "Let the Chart Spark: Embedding Semantic Context into Chart with Generative Model," *IEEE Trans. Vis. Comput. Graph.*, vol. 30, no. 1, pp. 284 – 294, 2024.
- [41] M. Mannino and A. Abouzied, "Expressive time series querying with hand-drawn scale-free sketches," in *Proc. ACM CHI*, 2018, pp. 1–13.
- [42] C. Zhou, C. C. Loy, and B. Dai, "Extract Free Dense Labels from CLIP," in *Proc. ECCV*, 2022, pp. 696–712.
- [43] Z. Li, Q. Ke, and W. Chen, "CLIP Guided Image-perceptive Prompt Learning for Image Enhancement," *arXiv preprint arXiv:2311.03943*, 2023.
- [44] X. Zhou, R. Girdhar, A. Joulin, P. Krähenbühl, and I. Misra, "Detecting Twenty-thousand Classes using Image-level Supervision," in *Proc. ECCV*, 2022, pp. 350–368.
- [45] R. Girdhar, A. El-Nouby, Z. Liu, M. Singh, K. V. Alwala, A. Joulin, and I. Misra, "Imagebind: One Embedding Space to Bind Them All," in *Proc. CVPR*, 2023, pp. 15180–15190.
- [46] S. Kantharaj, R. T. K. Leong, X. Lin, A. Masry, M. Thakkar, E. Hoque, and S. R. Joty, "Chart-to-Text: A Large-Scale Benchmark for Chart Summarization," in *Proc. ACL*, 2022, pp. 4005–4023.
- [47] Y. Ma, A. K. Tung, W. Wang, X. Gao, Z. Pan, and W. Chen, "ScatterNet: A deep subjective similarity model for visual analysis of scatterplots," *IEEE Trans. Vis. Comput. Graph.*, vol. 26, no. 3, pp. 1562–1576, 2018.
- [48] F. Lekschas, B. Peterson, D. Haehn, E. Ma, N. Gehlenborg, and H. Pfister, "Peax: Interactive Visual Pattern Search in Sequential Data Using Unsupervised Deep Representation Learning," *Comput. Graph. Forum*, vol. 39, no. 3, pp. 167–179, 2020.
- [49] Y. Ye, R. Huang, and W. Zeng, "VISAtlas: An image-based Exploration and Query System for Large Visualization Collections via Neural Image Embedding," *IEEE Trans. Vis. Comput. Graph.*, 2022.
- [50] T. Siddiqui, J. Lee, A. Kim, E. Xue, X. Yu, S. Zou, L. Guo, C. Liu, C. Wang, K. Karahalios *et al.*, "Fast-Forwarding to Desired Visualizations with Zenvisage," in *Proc. CIDR*, 2017.
- [51] Y. Luo, Y. Zhou, N. Tang, G. Li, C. Chai, and L. Shen, "Learned Data-aware Image Representations of Line Charts for Similarity Search," *Proc. ACMMOD*, vol. 1, no. 1, pp. 1–29, 2023.
- [52] J. J. Pan, J. Wang, and G. Li, "Survey of vector database management systems," *Proc. VLDB*, pp. 1–25, 2024.
- [53] A. Asai, S. Min, Z. Zhong, and D. Chen, "Retrieval-based Language Models and Applications," in *Proc. ACL*, 2023, pp. 41–46.
- [54] R. Guo, X. Luan, L. Xiang, X. Yan, X. Yi, J. Luo, Q. Cheng, W. Xu, J. Luo, F. Liu, Z. Cao, Y. Qiao, T. Wang, B. Tang, and C. Xie, "Manu: A Cloud Native Vector Database Management System," *Proc. VLDB*, vol. 15, no. 12, pp. 3548–3561, 2022.
- [55] J. Wang, X. Yi, R. Guo, H. Jin, P. Xu, S. Li, X. Wang, X. Guo, C. Li, X. Xu, K. Yu, Y. Yuan, Y. Zou, J. Long, Y. Cai, Z. Li, Z. Zhang, Y. Mo, J. Gu, R. Jiang, Y. Wei, and C. Xie, "Milvus: A Purpose-Built Vector Data Management System," in *Proc. ACM SIGMOD*, 2021, pp. 2614–2627.
- [56] "Chroma," <https://www.trychroma.com/>, accessed: 2024-03-20.
- [57] "Euclidesdb," <https://euclidesdb.readthedocs.io/en/latest/>, accessed: 2024-03-20.

- [58] C. Wei, B. Wu, S. Wang, R. Lou, C. Zhan, F. Li, and Y. Cai, "AnalyticDB-V: A Hybrid Analytical Engine Towards Query Fusion for Structured and Unstructured Data," *Proc. VLDB*, vol. 13, no. 12, pp. 3152–3165, 2020.
- [59] A. Radford, J. Wu, R. Child, D. Luan, D. Amodei, I. Sutskever *et al.*, "Language models are unsupervised multitask learners," *OpenAI blog*, vol. 1, no. 8, p. 9, 2019.
- [60] A. Dosovitskiy, L. Beyer, A. Kolesnikov, D. Weissenborn, X. Zhai, T. Unterthiner, M. Dehghani, M. Minderer, G. Heigold, S. Gelly, J. Uszkoreit, and N. Houlsby, "An image is worth 16x16 words: Transformers for image recognition at scale," in *Proc. ICLR*, 2021.
- [61] M. Eitz, J. Hays, and M. Alexa, "How Do Humans Sketch Objects?" *ACM Trans. Graph.*, vol. 31, no. 4, pp. 44:1–44:10, 2012.
- [62] R. Ma, H. Mei, H. Guan, W. Huang, F. Zhang, C. Xin, W. Dai, X. Wen, and W. Chen, "LADV: Deep Learning Assisted Authoring of Dashboard Visualizations From Images and Sketches," *IEEE Trans. Vis. Comput. Graph.*, vol. 27, no. 9, pp. 3717–3732, 2020.
- [63] R. Xia, B. Zhang, H. Peng, N. Liao, P. Ye, B. Shi, J. Yan, and Y. Qiao, "Structchart: Perception, structuring, reasoning for visual chart understanding," *arXiv preprint arXiv:2309.11268*, 2023.
- [64] F. Faghri, D. J. Fleet, J. R. Kiros, and S. Fidler, "VSE++: Improving Visual-Semantic Embeddings with Hard Negatives," in *Proc. BMVC*, 2018, p. 12.
- [65] J. S. Simonoff, *Smoothing methods in statistics*. Springer Science & Business Media, 2012.
- [66] J. Hao, Q. Shi, Y. Ye, and W. Zeng, "TimeTuner: Diagnosing Time Representations for Time-Series Forecasting with Counterfactual Explanations," *IEEE Trans. Vis. Comput. Graph.*, 2023.
- [67] H. Mouss, D. Mouss, N. Mouss, and L. Sefouhi, "Test of Page-Hinckley, an approach for fault detection in an agro-alimentary production system," in *Proc. IEEE ASCC*, vol. 2, 2004, pp. 815–818.
- [68] W. Chen, H. Wang, J. Chen, Y. Zhang, H. Wang, S. Li, X. Zhou, and W. Y. Wang, "TabFact: A Large-scale Dataset for Table-based Fact Verification," in *Proc. ICLR*, 2020.
- [69] M. E. Newman, "Power laws, Pareto distributions and Zipf's law," *Contemporary Physics*, vol. 46, no. 5, pp. 323–351, 2005.
- [70] B. Qin, B. Hui, L. Wang, M. Yang, J. Li, B. Li, R. Geng, R. Cao, J. Sun, L. Si *et al.*, "A survey on text-to-sql parsing: Concepts, methods, and future directions," *arXiv preprint arXiv:2208.13629*, 2022.
- [71] M. Cherti, R. Beaumont, R. Wightman, M. Wortsman, G. Ilharco, C. Gordon, C. Schuhmann, L. Schmidt, and J. Jitsev, "Reproducible Scaling Laws for Contrastive Language-Image Learning," in *Proc. CVPR*, 2023, pp. 2818–2829.
- [72] C. Fan, K. Matković, and H. Hauser, "Sketch-based fast and accurate querying of time series using parameter-sharing LSTM networks," *IEEE Trans. Vis. Comput. Graph.*, vol. 27, no. 12, pp. 4495–4506, 2020.
- [73] A. Gogolou, T. Tsandilas, T. Palpanas, and A. Bezerianos, "Comparing Similarity Perception in Time Series Visualizations," *IEEE Trans. Vis. Comput. Graph.*, vol. 25, no. 1, pp. 523–533, 2019.
- [74] Y. Yu, T. Becker, M. Behrisch *et al.*, "SAXRegEx: Multivariate time series pattern search with symbolic representation, regular expression, and query expansion," *Comput. Graph.*, vol. 112, pp. 13–21, 2023.
- [75] A. Joshi, S. Kale, S. Chandel, and D. K. Pal, "Likert Scale: Explored and explained," *BJAST*, vol. 7, no. 4, pp. 396–403, 2015.
- [76] M. Jin, S. Wang, L. Ma, Z. Chu, J. Y. Zhang, X. Shi, P.-Y. Chen, Y. Liang, Y.-F. Li, S. Pan, and Q. Wen, "Time-LLM: Time series Forecasting by Reprogramming Large Language Models," in *Proc. ICLR*, 2024.
- [77] D. Bromley and V. Setlur, "What Is the Difference Between a Mountain and a Molehill? quantifying semantic labeling of visual features in line charts," in *Proc. IEEE VIS*, 2023, pp. 161–165.
- [78] Y. Lin, H. Li, L. Yang, A. Wu, and H. Qu, "InkSight: Leveraging sketch interaction for documenting chart findings in computational notebooks," *IEEE Trans. Vis. Comput. Graph.*, 2023.
- [79] G. Shirato, N. Andrienko, and G. Andrienko, "Identifying, exploring, and interpreting time series shapes in multivariate time intervals," *Visual Informatics*, vol. 7, no. 1, pp. 77–91, 2023.
- [80] M. Daswani, M. M. J. Bellaiche, M. Wilson, D. Ivanov, M. Papkov, E. Schnider, J. Tang, K. Lamerigts, G. Botea, M. A. Sanchez, Y. Patel, S. Prabhakara, S. Shetty, and U. Telang, "Plots unlock time-series understanding in multimodal models," *arXiv preprint arXiv:2410.02637*, 2024.